Stimuli-Responsive Array of Microbeads Conjugated with Elastin-like Polypeptide

Jonghwan Lee¹, Jaeyeon Jung¹, Kyunga Na¹, Myeongjin Kim¹, Subeom Park¹, Pilwoo Heo² & Jinho Hyun¹

¹Department of Biosystems and Biomaterials Science and Engineering, Seoul National University, Seoul 151-742, Korea ²Energy Plant Team, Korea Institute of Machinery & Materials, Daejeon 305-343, Korea

Correspondence and requests for materials should be addressed to J. Hyun (jhyun@snu.ac.kr)

Accepted 7 October 2008

Abstract

It describes a platform of microarray for immunoassay using polystyrene microbeads (µbeads) conjugated with elastin-like polypeptides (ELP) as a responsive molecule to external stimuli. Prior to the highly resolved localization of µbeads for an array, photoresist micropatterns were fabricated onto the spun-cast adhesive thin layer. A UV-curable adhesive was applied to enhance the adhesion of µbeads to the substrate by controlling UV irradiation time. Spatial placement of µbeads on the photoresist micropatterns was easily performed with a flow of colloidal suspension through a device. The ubead array conjugated with ELP molecules was used for the immunoassay of prostate specific antigen (PSA), a cancer marker. The capture of PSA from a protein mixture was successful with high sensitivity and the release of PSA from the array was complete and reversible.

Keywords: Microarray, Microbead, ELP, Immunoassay, PSA

Introduction

In the paper, we describe a simple microfluidic bead -based immunoassay for detection of prostate-specific antigen (PSA). PSA is a 33 kDa serine protease that is produced by epithelial cells of the prostate gland¹. PSA has been used as a tumor marker for the monitoring of patients with prostate cancer. In serum, PSA exists in two different isoforms, free PSA (f-PSA) and complex PSA bound to α -1-antichymotrypsin (PSA-ACT)^{2,3}. Currently employed methods for

detection of PSA usually measure the total PSA level in serum and PSA value of 4.0 ng/mL is generally regarded as a cut-off value⁴. Besides the traditional immunoassay methods, several strategies have been developed for detection of PSA, including recombinant antibody⁵, binding peptide⁶, quantum dot⁷, carbon nanotube⁸, surface-enhanced Raman scattering (SERS)⁹, immuno PCR¹⁰, micro cantilever¹¹, microbead¹², and surface plasmon resonance (SPR)¹³. In addition to the fabrication methods, recent biochips have been requested to be functional for more rapid and accurate detection and analysis¹⁴. Among the materials to introduce a smart functionality to the biochips, elastin-like polypeptide (ELP) can be a potential candidate due to its effective and rapid separation and purification by simple phase transition. ELP containing repeats of the pentapeptide sequence Val-Pro-Gly-Xaa-Gly (VPGXG, where Xaa is any amino acid except Pro) has been previously identified as a smart biopolymer, as it undergoes a reversible phase transition in response to changes in temperature, pH, light, and ionic strength at its lower critical solution temperature (LCST)¹⁵⁻¹⁷. Characteristic hydrophobic-hydrophilic phase transition of ELP molecules by external stimuli enables the controllable and effective binding or separation of analytes from the surface^{18,19}. In the paper, the thermally controlled capture and release of PSA will be described using bead-based biochips functionalized with ELP.

Results and Discussion

By PCR and recursive directional ligation (RDL) method²⁰, an ELP molecule with repeating amino acid sequence of $\{[(VGPVG)_5]_8 + [(VGVPG)_{14} (KGVPG)]_8\}$ was synthesized and successfully purified by repetitive phase transition. The transition temperature (T_t) of ELP was determined to be 37°C by UV spectrometry, which meant that the ELP solution was transparent at temperatures below 37°C, but became turbid above 37°C due to the formation of ELP aggregates.

Sulfo-SANPAH is a heterobifunctional photoactivatable crosslinker containing amine-reactive NHS ester and photoactive nitrophenyl azide. Conjugation of ELP to polystyrene (PS) µbeads is achieved by reacting the amine groups of ELP with NHS groups on the PS µbead surface previously photocrossliked

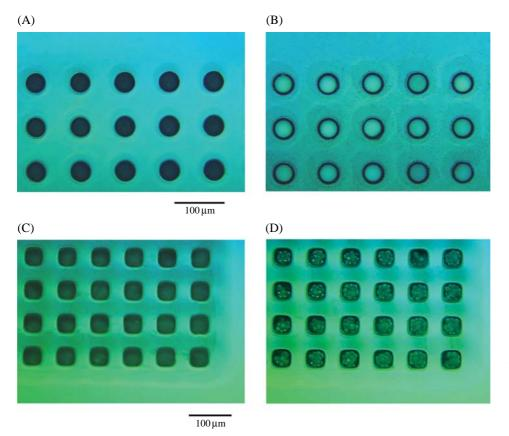


Figure 1. Optical images of ELP-PS μ bead microarrays. (A) 40 μ m circle features of photoresist micropatterns. (B) 30 μ m ELP-PS μ bead array in (A). (C) 40 μ m square features of photoresist micropatterns. (D) 10 μ m ELP-PS μ bead array in (C).

with Sulfo-SANPAH. The conjugation of ELP on the surface was confirmed by fluorescence detection using Alexa Fluor 488 conjugated ELP (data not shown). It is important to retain the responsiveness of ELP molecules attached on the surface for the reliable function in the system. Therefore, the stability of ELP-PS ubead against the changes of temperature, and ionic strength was evaluated. First, the stable attachment of ELP molecules on the ELP-PS µbeads was evaluated by changing its surrounding temperature up to 60°C. Second, the beads were immersed in various concentration of NaCl solution to observe the effect of salt concentration on the stability of ELP molecules bound to the bead surface. The fluorescence intensity was not decreased at high temperature and high salt concentration and confirmed the robust attachment on the surface (data not shown).

Figure 1A and 1C present the photoresist-micropatterned glass surface with exposed adhesive layer. UV-curable acrylate adhesive used in the experiment consisted of prepolymer, reactive monomer and photoinitiator and is generally applicable to paper, film, plastic, steel, wood, and glass surfaces. The UV curing reaction is induced by the absorption of UV light by the photoinitiator and subsequent free radical crosslinking of the resins. A UV-curable adhesive was spun-cast on the glass surface at 3,000 rpm for 30 sec and ~50 μ m thick layer was obtained by profilometer. The adhesive layer well covered the glass surface without any visible defect in the region by reflection microscopy and was cured by UV irradiation for micropatterning a photoresist on the surface. The UV dose of 40-140 mJ/cm² provided the good adhesion of the layer to the ELP-PS µbeads array even under ultrasonication with 50 : 50 (v/v) H₂O/ethanol mixture for 2 min. Moreover, the adhesion performance of the adhesive layer was maintained during photolithographic process.

Single- and multi-bead arrays of ELP-PS μ bead were spatially placed and immobilized onto the photoresist-micropatterned glass surface by a simple microfluidic flow of μ bead suspension. ELP-PS μ bead with various sizes could be successfully arrayed to the micropatterns by controlling the flow rate and evaporation process (Figure 1B, D). The adhesive layer on the bottom of micropatterns was important for the stable maintenance of arrayed μ bead-structures against the fast flow rate and evaporate rate.

PSA immunoassay was performed with the microfluidic ELP-PS µbeads array chip. At first, an ELP-

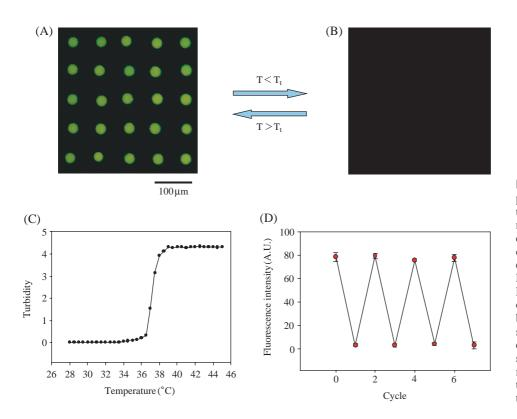


Figure 2. Reversible responsiveness of µbead arrays to thermal stimuli in immunoassay of PSA. Fluorescence images (A) after binding of Alexa Flour 488 conjugated secondary antiPSA to the ELP-PS µbeads array above LCST and (B) after removal of antigen-antibody complex below LCST. (C) Phase transition of ELP molecules according to temperature of solution. (D) Cyclic experiments in which the temperature was changed from 45°C to 10°C.

PS µbeads array was washed with fresh PBS buffer (pH 7.4) to remove any possible impurities on the surface. Then, the antiPSA-ELP conjugates were added to the ELP-PS µbeads array at the temperature above LCST of ELP to induce the specific binding of anti-PSA-ELP conjugate to the ELP-PS µbeads through the hydrophobic interactions between ELP molecules. Subsequently, unreacted antiPSA-ELP conjugates were removed with fresh 1M NaCl solution and the protein mixture composed of PSA, IgG, and BSA was added to the array. Unbound proteins were easily removed by washing the array twice with 1M NaCl solution. Fluorescence assay was performed by labeling PSA bound to the array with antibody-Alexa Fluor 488 conjugates in PBS buffer (pH 7.4) (Figure 2A).

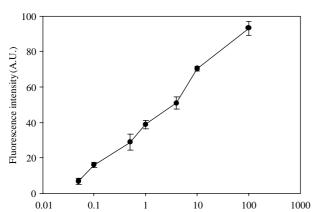
ELP-PS µbeads can be recovered by cooling the array to the temperature below the LCST of ELP. At the temperature below LCST, the hydrophobic interactions between ELP molecules disappeared and consequently, we could remove antigen-antibody complex from the ELP-PS µbeads array. The removal of antigen-antibody complex from the array was simply observed by fluorescence microscopy as shown in Figure 2B. The LCST of ELP used in this study was designed to close to the human body temperature (Figure 2C). The reversible phase transition of ELP molecules enabled the repetitive binding and removal of analytes with the arrays. 4 cyclic experiments showed

reliable smart property in specific binding of ELP-PS µbeads array (Figure 2D).

By utilizing the reversible phase transition of ELP, various concentrations of PSA molecules were successfully characterized and separated from the protein mixture. The dose response of ELP-PS µbeads array for the PSA immunoassay was shown in Figure 3. It showed linear relationship between the PSA concentration injected to the ELP-PS µbeads array and the fluorescence intensity measured from the ELP-PS µbeads array after PSA-antiPSA binding showing a minimum detection limit of 0.05 ng/mL. These results demonstrate the ELP-based assay systems as a reliable and promising detection tool for biomolecules.

Conclusions

It described a spatial localization of smart PS µbeads in the photoresist micropatterns and the highly selective detection of PSA by stimuli-responsiveness. The negative micropatterns of photoresist were fabricated on the curable adhesive layer and PS µbeads functionalized with ELP were placed with high resolution. The spatial localization of ELP-PS µbeads was successfully carried out by a simple flow of colloidal suspension. The ELP-PS µbeads in photoresist micropatterns were stable at harsh conditions of high tem-



PSA concentration (ng/mL)

Figure 3. Dose response curve for PSA detection.

perature and rapid flow rate of solutions. The controllable phase transition of ELP molecules enabled the reversible capture and release of PSA from the protein mixture inferring its reusability of devices as well as continuous analysis of multi-analytes with one biochip.

Materials and Methods

Construction and Characterization of ELP

Polymerase chain reaction (PCR) was performed to create a synthetic gene coding for (VGVPG)₅ (KGVPG) peptide sequence. ELP with various repeating peptide units have been constructed by employing RDL method²⁰. ELP expression was achieved by *E. coli* strain

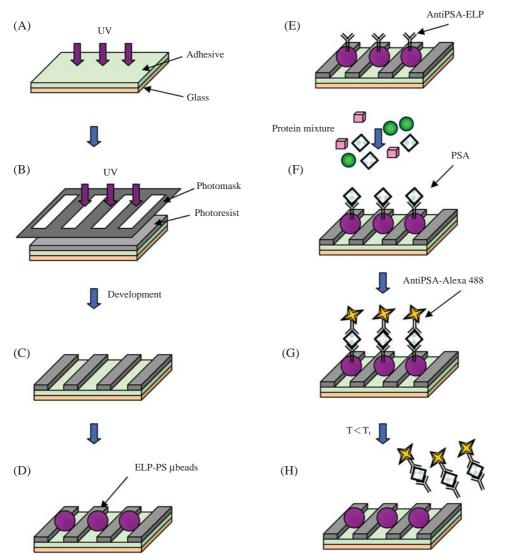


Figure 4. Schematic procedure for the fabrication of ELP-PS ubeads array and the smart immunoassay of PSA. (A) UV irradiation onto a spun-cast thin adhesive layer. (B) UV irradiation onto a spun-cast photoresist SU-8 2050 layer. (C) Removal of unexposed photoresist with SU-8 Developer. (D) ELP-PS µbeads array. (E) Binding of antiPSA-ELP conjugates to ELP-PS µbeads at the temperature above LCST. (F) Specific binding of PSA from protein mixture. (G) Binding of Alexa Flour 488 conjugated secondary antiPSA. (H) Release of antigen-antibody complex from ELP-PS µbeads by cooling to the temperature below LCST.

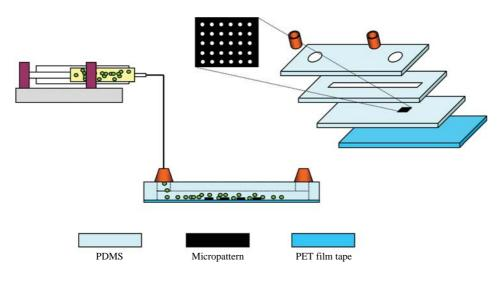


Figure 5. Schemetic representation of a microfluidic bead array chip.

BLR(DE3) (Novagen) using the modified pET-32b(+) vector (Novagen). All cultivation was carried out at 37°C in Circlegrow media (Q. Bio gene) supplemented with 100 µg/mL ampicillin. After 20 h of cultivation, cells were harvested and resuspended in PBS buffer (pH 7.4). The resuspended cells were lysed by sonication and cell debris was removed by centrifugation. Further purification of ELP was achieved by repetitive phase transition followed by ultracentrifugation as described previously²⁰. The T_t of purified ELP in PBS buffer (pH 7.4) was characterized by monitoring its absorbance at 350 nm using a UV-spectrophotometer, and was determined as the solution temperature at the half maximum of the turbidity gradient.

Preparation of ELP Conjugated PS μbead (ELP-PS μbead)

Suspensions of polystyrene microbead (PS µbead) with a diameter of 10 and 30 μ m (Polysiences, Inc. USA) were mixed with 0.5 mM N-sulfosuccinimidyl-6-[4'-azido-2'-nitrophenylamino] hexanoate (sulfo-SANPAH) (Pierce Chemical Co.) in 4 mL PBS buffer (pH 7.4) containing 0.5 mL dimethyl sulfoxide (DMSO). Photoactivation was performed by exposing the PS µbead suspension at 350 nm for 8 minutes. After the removal of unreacted reagents by centrifugation at 12,000 rpm for 15 min, 1 mL of 1 mM ELP solution in PBS buffer (pH 7.4) was added to the suspension. A crosslinking reaction between the SANPAH bound PS µbeads and ELP was performed for 2 h. The stability of ELP crosslinked to PS µbeads was investigated by changing incubation temperature and salt concentration using ELP labeled with the Alexa Fluor 488 conjugate (Invitrogen).

Fabrication of Photoresist Micropatterns on Adhesive Thin Layer

The UV-curable acrylate adhesive was coated onto a cleaned glass plate $(15 \times 15 \times 1 \text{ mm})$ using a spincoater at 3,000 rpm for 30 sec to make a uniform thin adhesive layer. The surfaces were then dried at room temperature for 2 to 5 min, and cured using a custombuilt UV curing equipment (~350 nm) by controlling the irradiation time and intensity (Figure 4A). The UV dose was measured with an IL 390C Light Bug UV radiometer (International Light, USA). The SU-8 2050 (MicroChem Corp.) photoresist was used to make a defined micropattern above the adhesive thin layer. Photoresist was poured onto the adhesive coated glass plate and spin coated at 2,000 rpm for 30 sec. The glass plate was then soft baked at 65°C for 1 min on the hot plate and 95°C for 5 min in the oven. The soft baked glass plate was then slowly cooled down to room temperature and was exposed to UV radiation through the photomask (Figure 4B). The micropatterned glass plate was then hard baked at 95 °C for 8 min in the oven and followed by immersed in SU-8 Developer (MicroChem Corp.) (Figure 4C). After the development process, the stickiness of the exposed adhesive layer was characterized with a probe tag test using the TAXT2i texture analyzer (Stable Micro Systems, UK) and a cylindrical probe. The test was performed with a contact force of 100 g/cm^2 , a contact time of 1 sec, and a 5 mm/sec debonding rate; the stickiness was determined as the debonding force.

Fabrication of a Bead Array Chip

The µbead array chip consisted of photoresist-micropatterned glass surface, poly(dimethylsiloxane) PDMS layer, and polyethylene terephthalate (PET) film tape (Figure 5). We have employed simple microfluidic method to make a spatially localized array of ELP-PS µbead onto the micropatterned glass surface. The suspension of ELP-PS µbead in PBS buffer (pH 7.4) was introduced into the device using microsyring pump connected to the inlet tubing. Spatial arrangement of ELP-PS µbead was controlled by flow rate, concentration of bead suspension, and evaporation rate (Figure 4D).

Smart Immunoassay of PSA

A 50 fold-dilution of antiPSA (Invitrogen) in PBS buffer (pH 7.4) was activated with 5 mM N-hydroxysuccinimide (NHS) and 2 mM 1-ethyl-3-(dimethylaminopropyl) carbodiimide hydrochloride (EDC) and subsequently mixed with 10 µM ELP solution in PBS buffer (pH 7.4) for molecular conjugation (antiPSA-ELP). AntiPSA-ELP conjugates were then added to the ELP-PS ubead and the temperature was raised above the T_t of the conjugated ELPs (Figure 4E). Anti-PSA-ELP that had not bound to the ELP-PS µbead array was removed by washing the array with a 1 M NaCl solution. Subsequently, the protein mixture composed of PSA, IgG, and BSA was then introduced to the the ELP-PS µbead array and washed with 1 M NaCl (Figure 4F). Finally, Alexa Fluor 488 conjugated secondary antibodies were added and the bead array was visualized using fluorescence microscopy (BX21, Olympus, Japan) (Figure 4G). The release of analytes from the array surface was performed by washing the array with ice-cold PBS buffer (pH 7.4) (Figure 4H).

Acknowledgements

This work was supported by grant from Korea Institute of Machinery and Materials. The authors acknowledge support from a grant from the Research Institute for Agriculture and Life Sciences in Seoul National University.

References

- 1. Watt, K.W.K., Lee, P.J., M'Timkulu, T., Chan, W.P. & Loor, R. Human prostate-specific antigen: structural and functional similarity with serine proteases. *Proc. Natl. Acad. Sci.* **83**, 3166-3170 (1986).
- Stenman, U.H. *et al.* A complex between prostatespecific antigen and alpha 1-antichymotrypsin is the major form of prostate-specific antigen in serum of patients with prostatic cancer: assay of the complex improves clinical sensitivity for cancer. *Cancer Res.* 51, 222-226 (1991).

- 3. Lilja H. Significance of different molecular forms of serum PSA. the free, noncomplexed forms of PSA versus that complexed to alpha 1-antichymotrypsin. *Urol. Clin. North. Am.* **20**, 681-686 (1993).
- Catalona, W.J., Smith, D.S., Ratliff, T.L. & Basler, J.W. Detection of organ-confined prostate cancer is increased through prostate-specific antigen-based screening. *JAMA*. 270, 948-954 (1993).
- Harma, H., Tarkkinen, P., Soukka, T. & Lovgren, T. Miniature single-particle immunoassay for prostatespecific antigen in serum using recombinant Fab fragments. *Clin. Chem.* 46, 1755-1761 (2000).
- 6. Wu, P., Stenman, U.H., Pakkala, M., Narvanen, A. & Leinonen, J. Separation of enzymatically active and inactive prostate-specific antigen (PSA) by peptide affinity chromatography. *The Prostate* **58**, 345-353 (2004).
- Wang, J., Liu, G., Wu, H. & Lin, Y. Quantum-dotbased electrochemical immunoassay for high-throughput screening of the prostate-specific antigen. *Small* 4, 82-86 (2008).
- 8. Briman, M. *et al.* Direct electronic detection of prostate-specific antigen in serum. *Small* **3**, 758-762 (2007).
- Grubisha, D.S., Lipert, R.J., Park, H.Y., Driskell, J. & Porter, M.D. Femtomolar detection of prostate-specific antigen: an immunoassay based on surface-enhanced raman scattering and immunogold labels. *Anal. Chem.* **75**, 5936-5943 (2003).
- Lind, K. & Kubista, M. Development and evaluation of three real-time immuno-PCR assemblages for quantification of PSA. J. Immunol. Methods 304, 107-116 (2005).
- Wee, K.W. *et al.* Novel electrical detection of labelfree disease marker proteins using piezoresistive selfsensing micro-cantilevers. *Biosen. Bioelectron.* 20, 1932-1938 (2005).
- Kim, Y.J., Kim, H.Y., Ah, C.S., Jung, M.Y. & Park, S.H. Some key factors in a bead-based fluorescence immunoassay. *BioChip J.* 2, 60-65 (2008).
- Besselink, G.A.J., Kooyman, R.P.H., van Os, P.J.H.J., Engbers, G.H.M. & Schasfoort, R.B.M. Signal amplification on planar and gel-type sensor surfaces in surface plasmon resonsnace-based detection of prostate-specific antigen. *Anal. Biochem.* 333, 165-173 (2004).
- Vo-Dinh, T., Griffin, G., Stokes, D.L. & Winterberg, A. Multi-functional biochip for medical diagnostics and pathogen detection. *Sens. Act. B* **90**, 104-111 (2003).
- Alonso, M., Reboto, V., Guiscardo, L., Mate, V. & Rodriguez-Cabello, J.C. Novel photoresponsive pphenylazobenzene derivative of an elastin-like polymer with enhanced control of azobenzene content and without pH sensitiveness. *Macromolecules* 34, 8072-8077 (2001).
- 16. Urry, D.W. Physical chemistry of biological free energy transduction as demonstrated by elastic pro-

tein-based polymers. J. Phys. Chem. B 101, 11007-11028 (1997).

- 17. Girotti, A. *et al.* Influence of the molecular weight on the inverse temperature transition of a model genetically engineered elastin-like pH-responsive polymer. *Macromolecules* **34**, 3396-3400 (2004).
- 18. Gao, D. *et al.* Fabrication of antibody arrays using thermally responsive elastin fusion proteins. *J. Am. Chem. Soc.* **128**, 676-677 (2006).
- Banki, M.R., Feng, L. & Wood, D.W. Simple bioseparations using self-cleaving elastin-like polypeptide tags. *Nature Methods* 2, 659-661 (2005).
- Meyer, D.E. & Chilkoti, A. Genetically encoded synthesis of protein-based polymers with precisely specified molecular weight and sequence by recursive directional ligation: examples from the elastin-like polypeptide system. *Biomacromolecules* 3, 357-367 (2002).